

Indian monsoon variability in the last 2000 years as inferred from benthic foraminifera

Thejasino Suokhrie, S. M. Saalim, R. Saraswat*, R. Nigam

Micropaleontology Laboratory, Geological Oceanography Division,

National Institute of Oceanography, Goa, India

* For Correspondence: rsaraswat@nio.org

Abstract

The effect of ambient conditions on living (Rose-Bengal stained) benthic foraminifera has been studied from the shelf and slope of central-western Bay of Bengal to assess the applicability of temporal changes in benthic foraminiferal morpho-groups (angular asymmetrical and rounded symmetrical) to reconstruct past monsoon changes. We report that the riverine influx and associated processes control the relative abundance of angular asymmetrical (AABF) and rounded symmetrical (RSBF) benthic foraminiferal morpho-groups in the central-western Bay of Bengal. Subsequently, temporal variations in relative abundance of AABF in a gravity core collected from outfall region of Pennar River, are used to reconstruct decadal scale past monsoon variability during the last ~1887 years. An increased monsoon discharge is observed during Medieval Warm Period (MWP) and lower during Little Ice Age (LIA). The periodic changes with a frequency of ~123 and ~238 years are also identified, indicating a close relationship between monsoon and solar activity.

Keywords: Benthic foraminifera, Morpho-group, Ecology, Indian monsoon, Bay of Bengal

1.Introduction

About 65% of the major produce in India comes from agriculture (Gadgil, 1999) and it is highly dependent on the monsoon rainfall. Minor changes in rainfall result in severe drought in many parts of the country and a drop in food production and gross domestic product (Gadgil, 2004). Hence, prediction of future trends in monsoon is necessary for sustainable development. Monsoon prediction requires proper understanding of monsoon dynamics. Even though the effect of various regional and global processes on Indian monsoon is known (Halley, 1686; Charney, 1969; Chao and Chen, 2001; Gadgil, 2003; Wang et al., 2009), the inconsistent relationship (Kumar et al., 1999) hampers proper monsoon prediction. Additionally, long-term trends in monsoon variability are also hard to infer from limited instrumental data (Goswami, 2006). The knowledge of the past monsoon can help in understanding long-term trends in monsoon behavior under various boundary conditions (Clift and Plumb, 2008; Mohtadi et al., 2014). Various proxies from both continent and marine environment have helped in the reconstruction of past monsoon (Henderson, 2002, Staubwasser and Weiss, 2006; Clift and Plumb, 2008; Achyuthan et al., 2013; Bradley, 2014; Mohtadi et al., 2014; Saraswat et al., 2014; 2015). Proxies from the marine environment, in particular, offer long, continuous and uninterrupted records.

Several attempts have been made to reconstruct past monsoon from the northern Indian Ocean by using both faunal census (Clemens and Prell, 1991; Nigam et al., 1992; Nigam et al., 1995; Naidu and Malmgren, 1996; Gupta et al., 2003; 2005; Saraswat et al., 2005; Singh et al., 2011; 2014; Saraswat et al., 2016) and other proxies (Sirocko et al., 1993; Kudrass et al., 2001; Chauhan, 2003; AnilKumar et al., 2005; Tiwari et al., 2005; Govil and Naidu, 2011; Saraswat et al., 2012; 2013; Kessarkar et al., 2013; Mahesh and Banakar, 2014; Mohtadi et al., 2016; Sijinkumar et al., 2016). A majority of these records were based on cores collected from regions with comparatively low sedimentation rate and thus had centennial to multi-centennial resolution. The reconstruction of past monsoon from high sedimentation rate areas can help to generate sub-centennial to decadal resolution records that can help in understanding short-term monsoon variability. A huge amount of sediment discharge in the Bay of Bengal provides an ideal location to reconstruct high-resolution paleo-monsoon records. High resolution sub-centennial to decadal resolution records from the core monsoon region of the northern Bay of Bengal are, however, limited mainly because of the sparse presence of planktic foraminifera (Kudrass et al., 2001; Chauhan, 2003; Rana and Nigam, 2009; Rashid et al., 2011; Panchang and Nigam, 2012; Ponton et al., 2012). The abundant presence of benthic foraminifera in these sediments can help to reconstruct high-resolution past monsoon changes. Earlier, temporal changes in benthic foraminiferal morpho-groups, namely angular

asymmetrical benthic foraminifera and rounded symmetrical benthic foraminifera were suggested as a proxy to reconstruct past monsoon from the riverine influx dominated continental shelf regions of the Arabian Sea (Nigam et al., 1992). The application of benthic foraminiferal morpho-groups for paleoclimatic studies stemmed from their preference for characteristic ambient conditions, especially depth (Severin, 1983), organic carbon (Corliss and Chen, 1988) and dissolved oxygen concentration (Bernhard, 1986; Kaiho, 1991; Nigam et al., 2007; Mazumder and Nigam, 2014). The relationship between a particular morpho-group and ambient environment, however, may vary regionally. The western Bay of Bengal is ideal to assess the applicability of such benthic foraminiferal morpho-groups to reconstruct past monsoon and use it to reconstruct decadal resolution monsoon changes.

2. Study Area

The study area is in the central-western Bay of Bengal and covers major rivers, namely Krishna-Godavari, Pennar and Kaveri (Fig 1). The Bay of Bengal is the largest bay in the world and forms the north-eastern part of the Indian Ocean. The hydrographic parameters in the Bay of Bengal are strongly influenced by the seasonally reversing monsoon currents and resulting immense fresh water run-off (during southwest monsoon freshwater discharge is $183 \times 10^{11} \text{ m}^3$) (Varkey et al., 1996). The sediment accumulation in this river dominated bay is huge (1350 million tons/yr, Milliman, 2001). This freshwater influx combined with the monsoon winds strongly influences surface water circulation and stratification (Gomes et al., 2000). The freshwater influx reduces the surface water salinity by ~ 7 psu in the northern bay (Levitus et al., 1994) and enhances primary productivity by increasing nutrient supply (Ramaswamy and Nair, 1994). However, biological productivity in the Bay of Bengal is comparatively lower than in the Arabian Sea due to strong stratification, more cloud cover and turbidity (Prasanna Kumar et al., 2010). The eddy pumping mechanism in the Bay of Bengal has, however, explained how the biological productivity is enhanced (Ostlund et al., 1980, Prasanna et al., 2004) resulting in comparable annual organic flux with that of Arabian Sea (Ramaswamy and Nair, 1994). The distribution of oxygen is influenced by physical processes like freshwater influx, upwelling, atmospheric interaction, water mass transport and biological processes like photosynthesis and respiration. In the Bay of Bengal, the waters experience intense oxygen depletion at intermediate depths of 200–800 m resulting in a pronounced oxygen minimum zone (OMZ), with the resultant dissolved oxygen content as low as $>5 \mu\text{M}$ (Wyrski, 1971; Rao et al., 1994; Sardessai et al., 2007). The uptake and demand for oxygen in the bay, however, does not lead to hypoxic conditions as in Arabian Sea which is known for its OMZ and de-nitrification (de Sousa et al., 1996; Naqvi et al., 2000). The salinity at the sediment-water interface is low in front of the river mouth and increases towards the slope (Fig. 2). The seawater temperature at the same interface

is, however, much higher in the shelf region and decreases considerably towards the deeper region (Fig. 2). The range of seawater temperature at the sediment-water interface is much large as compared to the salinity. The dissolved oxygen is comparatively lower in the upper part of the study area (Fig. 2).

Materials and Methods

A total of 46 surface sediment samples and a gravity core collected from the western Bay of Bengal were used (Fig. 1, Table 1). The surface sediments comprised of 35 multi-core top (SK308 MC-02 to MC-38) and 11 spade-core top (SSK35 SC-37 to SC-46) samples covering a depth range from 27 m to 2494 m. The salinity and temperature of the overlying bottom water were measured onboard at all the 35 multicore stations using a hand held multimeter (model number: S47-K/'SevenMulti'). The environmental data (salinity and temperature) for the 11 spade core stations as well as dissolved oxygen concentration at all stations (both multi-core and spade core) was extracted from World Ocean Circulation Experiment (WOCE), Global Hydrographic Climatology 2009 (Gouretski and Koltermann, 2004) using Ocean Data View software 4 version (Schlitzer, 2016). The gravity core (SK308 GC-02) was collected off Pennar River (14°34.115' N, 80°35.112' E, and 2094 m water depth) (Table 2). The top 120 cm of the core, sub-sampled at 1 cm interval, was used to reconstruct past monsoon.

The surface sediment samples were preserved in Rose-Bengal stain (2 g Rose-Bengal per liter of 99.9% ethanol) for a minimum of two weeks to differentiate living (stained) from the dead (unstained) foraminifera. The sediment samples were processed following the standard processing technique of soaking in distilled water overnight followed by washing through a 63 µm sieve using a slow shower. A minimum of 300 living, as well as 300 dead benthic foraminifera, were picked from a representative aliquot obtained by coning and quartering the dried >63 µm coarse fraction (CF). In samples with a limited number of living specimens, a fixed weight of 0.1 g was taken for picking. To decrease the discrepancy in picking Rose-Bengal stained living benthic foraminifera, only those specimens with clear pink colouration and tests with more than one chamber completely stained were picked and counted. From the picked benthic assemblage, angular asymmetrical benthic foraminifera (AABF) were counted based on the external morphology, following the criteria of Severin, (1983) and Nigam et al., (1992). This parameter is well established and widely used as a proxy for paleomonsoon intensity in regions near the riverine influx (Nigam et al., 1992). Additionally, rounded symmetrical benthic foraminifera (RSBF) were also counted. The distribution pattern of AABF and RSBF was compared with the ambient environmental data. A statistical analysis,

Principal Component Analysis (PCA) was performed to understand and limit the influence of the more significant environmental parameter on the relative abundance of AABF and RSBF.

The core samples were processed following the same method as the surface sediment samples. The age model of the gravity core SK308 GC-02, was established by using three accelerator mass spectrometer (AMS) ^{14}C dates measured on mixed planktic foraminifera picked from $>63\ \mu\text{m}$ fraction (Table 3). AMS dating was carried out at the Centre for Applied Isotopic Studies, University of Georgia, USA. The ^{14}C ages were then calibrated by using Marine13 dataset (Reimer et al., 2013) from the online calibration program Calib7.1 version (Stuiver and Reimer, 2016). The average reservoir correction (ΔR) of 108 ± 208 yr for Pondicherry, India (12.1°N 80°E ; Southon et al., 2002), Rameswaram, Tamil Nadu (9.17°N 79.22°E ; Dutta et al., 2001) and Mandapam, Tamil Nadu, (9.2°N 78.7°E ; Dutta et al., 2001) was applied to calibrate radiocarbon dates. Considering the top to be intact, it was assigned to the year 2014 (year of sample collection). The dates of all other samples were calculated assuming constant sedimentation rates in between and thereby linearly interpolating the values. The sample resolution was 13 yr/cm in the top 100 cm of the core and 24 yr/cm for the rest of the core till 120 cm. Thus, the core covers a time span from 226 AD till 2014 AD representing ~1887 years. AABF and RSBF were counted from a representative aliquot obtained by coning and quartering the $>63\ \mu\text{m}$ sieved coarse fraction and the percentages were calculated for each sample. The down-core variation in the relative abundances of AABF, RSBF and coarse fraction (%CF) were used to reconstruct paleomonsoon changes. Spectral analysis of AABF was performed using REDFIT 3.5 program (Schultz and Mudelsee, 2002) to verify if there is any cyclicity in climatic events.

Results

1.1. Organic Carbon ($\%C_{\text{org}}$)

Organic carbon is low in the inner shelf region and increases towards the slope (Fig. 3). A comparatively higher $\%C_{\text{org}}$ is observed in the region north of Godavari River. Another patch of higher $\%C_{\text{org}}$ is also observed in the slope region in front of both the Krishna and Pennar River.

1.2. Coarse fraction ($>63\ \mu\text{m}$) ($\%CF$)

The $\%CF$ in the study area is the highest at SC-45 (96.4%) and lowest at MC-24 (0.09%). The $\%CF$ increases from the shallow depth towards the deep. The trend of increase in $\%CF$ away from the shallow depth holds true in all the stations lying in the vicinity of the rivers, except for stations falling in between the river mouth. Also, the southern segment of the study area exhibited higher $\%CF$ (Fig. 4).

1.3. Ecology of morpho-groups

Benthic foraminifera were grouped into AABF and RSBF (Figure 5). The relative abundance of fossil AABF is the maximum (95%) at SC-36 (145 m water depth) and the living AABF accounted for up to 100% of total benthic foraminifera at MC-04 (978 m water depth). The relative abundance of both fossil and living AABF is comparable (Fig. 6, Table 1). The relative abundance of AABF increases towards the deeper locations, i.e. away from the river mouths. These deeper depth locations in the study area represent a calmer and more saline environment, with colder and less oxygenated waters. The relative abundance of fossil RSBF in surface sediment samples is the maximum (75%) at SC-40 (53 m water depth) and that of living RSBF is maximum at SC-41 (61 m water depth). The relative abundance of RSBF is higher towards the shallow depth (Fig. 6) and closer to the major riverine systems like Godavari-Krishna and Pennar rivers. The abundance is also high, right at the river mouths (SC-40, MC-28, MC-29 and MC-07) than in the region in-between the river mouths. The salinity is low in the shallower depths near river mouths (Krishna-Godavari, Pennar and Cauvery) and a comparison with the relative abundance of AABF indicates direct relationship, suggesting that this morpho-group favours hypersaline water. Additionally, the DO decreases towards the deeper depths where relative abundance of AABF is high, suggesting an inverse relationship between the two (Fig. 2).

1.4. Principal Component Analysis

For a better and more reliable interpretation of the relationship of the AABF and RSBF relative abundance with the ambient environmental parameters, (bottom water depth, temperature, DO, salinity and %C_{org}), principal component analysis was performed (Fig. 7, Table 4). Here, the foraminiferal data was taken as independent variable while all the other measured environmental parameters were taken as dependent variable. The reliability of the obtained data was measured by a standard value called the statistical significance level (p-value/level). The correlations are considered statistically significant at $p < 0.05$. Bottom water temperature shows significant positive relation ($r^2 = 0.4$) with AABF. Bottom water DO and temperature has a negative relation ($r^2 = -0.37$ and -0.52 , respectively) with AABF abundance. However, bottom water DO does not have significant control on the abundance. %CF and bottom water salinity does not show any significant relation with AABF abundance.

1.5. Subsurface Signatures:

Coarse fraction

The %CF in the core (SK308 GC-02) varies from a minimum of 0.2% at ~734 AD (99-100 cm) to a maximum of 1.4% at ~1762 AD (19-20 cm) (Fig. 8). The %CF prior to ~1762 AD was more or less constant; however, an increase began by ~1670 AD reaching a peak at ~1762 AD. This increase in %CF was followed by a gradual descent. The %CF began to increase again from ~1900 AD onwards and continued till present.

Angular Asymmetrical Benthic Foraminifera (AABF)

The relative abundance of AABF fluctuates throughout the core (Fig. 8). The maximum and more amplified fluctuations are observed before ~1201 AD, as compared to the ages afterward. The lowest abundance of AABF (29%) is at ~885 AD (87-88 cm) and the highest (92%) is at ~589 AD (105-106 cm). Prominent peaks in relative abundance of AABF are observed at ~323 AD (116-117 cm), ~589 AD (105-106 cm), ~734 AD (99-100 cm), ~848 AD (90-91 cm), ~961 AD (81-82 cm) then again at ~1100 AD (70-71 cm), ~1201 AD (62-63 cm), ~1302 AD (54-55 cm), ~1431 AD (44-45 cm), ~1630 AD (29-30 cm), and also at ~1935 AD (6-7 cm). It is also noteworthy to mention that the AABF percentage is inversely related to the %CF percentage throughout the core, with higher abundance of AABF correlating with lower %CF (Fig 6). This relation is clearly seen at ~885 AD and during the period between ~1650 AD to ~1750 AD where the %CF spikes up to a maximum level while the AABF percentage shows a decreasing trend (Fig. 8).

Rounded Symmetrical Benthic Foraminifera (RSBF)

The relative abundance of RSBF in the core ranges from a minimum of 8% at ~589 AD (105-106 cm) to a maximum of 71% at ~885 AD (87-88 cm). In surface sediments, RSBF are abundant at the shallower depths, particularly at the mouth of the rivers where higher energy conditions prevail. In the core, the higher abundances of RSBF correlates well with, the higher %CF (Fig. 8).

Discussion

1.6. Ecology of benthic foraminiferal morpho-groups

The relative abundance of AABF in the surface sediments from the shelf and slope of the central-western Bay of Bengal increases away from the shallow depth indicating its preference for hypersaline, calmer and less oxygenated colder water. Therefore, in the central-western Bay of Bengal, AABF relative abundance is directly related to salinity. Further, the %CF has an inverse relationship with the AABF abundance indicating their preference for finer substrate deposited in

low energy environment. From the PCA plot (Fig. 5, Table 3), it is clear that there is significant preference of AABF to deeper water depth where the temperature is comparatively lower than the shallow water depth. In view of the absence of a direct parameter to measure the bottom water energy at different stations, the depth can be used as an indicator of bottom water energy condition. The increased relative abundance of AABF at deeper depths, away from the river mouth, therefore, suggests its preference for low energy, cold water. This is in accordance with previous reports from the Arabian Sea (Nigam et al., 1992) as well as from northern Bay of Bengal (Manasa et al., 2016). The statistically insignificant relationship with bottom water salinity is attributed to the small difference in bottom water salinity at various stations, as compared to the large difference in seawater temperature. The freshwater influx dominated upper water column in the Bay of Bengal is warmer than the layers below (Durand et al., 2011). The foraminiferal response to temperature in the western Bay of Bengal, therefore can also be attributed to the freshwater influx. Therefore, in the shelf and slope of the central-western Bay of Bengal, the higher AABF abundance is suggestive of reduced freshwater influx during weak monsoon periods. Even though the DO concentration does not seem to significantly influence AABF abundance, the DO concentration is low at deeper water depth. The temporal changes in the relative abundance of morpho-groups as a proxy for freshwater influx and hence monsoon intensity has been widely used to reconstruct paleomonsoon fluctuations from the Arabian Sea (Nigam et al., 1992). As the volume of freshwater and material influx of the rivers draining into the Bay of Bengal is higher, it is necessary to assess the applicability of the same in river-dominated central-western Bay of Bengal. The preference of AABF to oxygen-depleted environments has also been reported by various workers (Sen Gupta and Machain-Castillo 1993; Nigam et al. 2007; Schumacher et al. 2007; Nagy et al. 2009; Caille et al. 2014). We infer from the modern distribution of relative abundance of AABF, that, the higher percentage of AABF indicates less freshwater influx and hence weaker monsoon, lesser turbulence, and less coarse material.

1.7. Past Monsoon Changes

The ecology of AABF as inferred from the surface sediments points out to its preference to deeper depth locations having low and calmer energy conditions with less oxygenated, cooler and more saline water. With this knowledge, it can be inferred that the various peaks of AABF relative abundance throughout the core indicate periods of lesser terrigenous influx and further to periods of reduced monsoonal precipitation. Additionally, the %CF in the core is a reflection of the energy condition wherein, the increase in %CF can be related to higher energy conditions. The more coarse material is brought to the continental margins, because of high precipitation as it brings more terrigenous sediments through freshwater influx. A comparison of the AABF and %CF suggests an

inverse relationship with each other. The above-mentioned relationship between AABF and %CF holds true considering the vicinity of the core to the Pennar River mouth. The %CF tends to be higher (lower) and AABF lower when the freshwater input is more (less) due to intense (weak) monsoon.

The observed peaks in AABF record thus indicate dry periods or periods of comparatively less monsoon precipitation. An increasing trend of AABF from ~372 to ~589 AD with an exception at ~493 AD suggests lesser terrigenous influx and implies a weakening of monsoon precipitation during that period. An abrupt decrease from ~589 AD to ~637 AD and an abrupt increase from ~637 to ~734 AD respectively may indicate rapid strengthening and weakening of monsoon. This inference is also supported by respective increase and decrease in %CF during the same period. An overall decreasing trend of AABF from ~734 AD onwards till ~1251 AD (Fig. 7), except for a prominent peak at ~1201 AD, imply an increasing trend of monsoon precipitation. A period of minimum AABF (~885-993 AD) with corresponding high %CF (~885-923 AD) indicates the period of maximum monsoon influx. An abrupt increase in AABF with peaks at ~1431, 1524, and 1630 AD signifying an abrupt decrease in monsoon influx marked the beginning of Little Ice Age (Fig. 9). Other records from Arabian Sea (Agnihotri et al., 2002, Gupta et al., 2003), stalagmite records from Oman and Yemen (Burns et al., 2002, Fleitmann et al., 2007), pollen records from western Himalaya (Phadtare and Pant, 2006), also reported relatively warmer and wetter climate during Medieval Warm Period (MWP) as compared to weaker monsoon during Little Ice Age. The inference of weaker monsoon intensity during LIA from our record is also supported by speleothem records from Dandak Cave in Central India (Sinha et al., 2007) as well as planktic foraminiferal records from the Arabian Sea (Tiwari et al., 2005 Agnihotri et al., 2002). All of these records reported drier conditions implying lesser monsoonal rainfall during LIA. Similar weaker monsoon during Little Ice Age has also been reported from other parts of the world, including speleothem records from Wanxiang Cave (Zhang et al., 2008) and tree ring records from southern Vietnam (Buckley et al., 2010). Except for a decrease at ~1683 AD, ~1736 AD and again at ~1762 AD, the overall increasing trend of AABF appears to continue till ~1935 AD. The decrease in AABF at ~1683 AD, ~1736 AD and ~1762 AD is also observed in foraminiferal records off Myanmar (Panchang et al., 2012) where a low salinity indicator species was used to delineate freshwater pulses at ~1675, 1750 and 1850 AD.

1.8. Cyclicity

The AABF relative abundance dataset was analyzed for cyclicity using the software Redfit 3.4, to find out if any periodicity exists in climatic events. The AABF dataset revealed a ~123 and ~238 years cyclicity at 95% and 90% level of significance, respectively (Fig. 10). As also can be visually

observed (Fig. 7), the most prominent cycles range from 101 to 150 years. These cycles may be related to various climate forcing factors or feedback mechanisms such as solar cycles. The observed ~123 and ~238 year periodicity closely match the periodicities of sunspot numbers (117, 132, 150, 209, 226 years), indicating a good relationship between solar activity and monsoonal processes also reported in other previous studies (Agnihotri et al., 2002, Tiwari et al., 2005, Wang et al., 2005, Gupta et al., 2005, Rana et al., 2009).

Conclusions

The factors controlling the relative abundance of angular asymmetrical and rounded symmetrical benthic foraminiferal morpho-group have been evaluated from the central western Bay of Bengal. We report that riverine influx and associated changes affect the spatial variation in relative abundance of benthic foraminiferal morpho-groups. The technique was then applied on gravity core SK308 GC-02 recovered off Pennar river mouth, where the river discharge is majorly controlled by monsoonal precipitation. The AABF and %CF variations were found to be almost inversely related; higher AABF corresponding to lower %CF, suggesting weaker monsoon and vice versa. A general, increasing trend of monsoonal discharge was observed during the MWP (~734 -1251 AD) except at ~1201 AD, and decreased monsoonal discharge during LIA (peaks at ~1431, 1524, and 1630 AD), continuing till present with some minor fluctuations. The AABF dataset exhibited prominent ~123 and ~238 years cyclicity which is very indicative of a strong relationship of monsoon with solar activity.

Acknowledgements

Authors are thankful to the Ministry of Earth Sciences, India for funding a project under SIBER program. TS is thankful to the University Grants Commission (UGC), India for providing Senior Research Fellowship. Authors are thankful to Ms. Viola R. (NIO) for her help in performing spectral analysis. Authors also acknowledge the financial support by CSIR, India to GEOSINKS project and Dr. B. Nagender Nath for providing the spade core samples and the help at various stages. We also thank Dr. C. Prakash Babu, National Institute of Oceanography, India for the help in organic carbon analysis.

References

- Achyuthan, H., Deshpande, R.D., Rao, M.S., Kumar, B., Nallathambi, T., Shashi Kumar, K., Ramesh, R., Ramachandran, P., Maurya, A.S., Gupta, S.K., 2013. Stable isotopes and salinity in the surface waters of the Bay of Bengal: Implications for water dynamics and palaeoclimate. *Marine Chemistry*, 149, 51-62.
- Agnihotri, R., Dutta, K., Bhushan, R., Somayajulu, B.L.K., 2002. Evidence for solar forcing on the Indian monsoon during the last millennium. *Earth Planetary Science Letters* 198, 521–527.
- AnilKumar, K., Rao, V.P., Patil, S.K., Kessarkar, P.M., Thamban, M., 2005. Rock magnetic records of the sediments of the eastern Arabian Sea: Evidence for the late Quaternary climatic change. *Marine Geology* 220, 59-82.
- Antonov, J.I., Seidov, D., Boyer, T.P., Locarnini, R.A., Mishonov, A.V., Garcia, H.E., Baranova, O.K., Zweng, M.M., Johnson, D.R., 2010. *World Ocean Atlas 2009, Volume 2: Salinity*. S. Levitus, Ed. NOAA Atlas NESDIS 69, U.S. Government Printing Office, Washington, D.C., 184.
- Bernhard, J.M., 1986. Characteristic assemblages and morphologies of benthic foraminifera from anoxic, organic-rich deposits: Jurassic through Holocene. *Journal of Foraminiferal Research* 16, 207-215.
- Bradley, R.S., 2014. *Paleoclimatology: Reconstructing Climates of the Quaternary* (3rd edition). Elsevier/Academic Press, San Diego, 675 pp.
- Buckley, B.M., Anchukaitis, K.J., Penny, D., Fletcher, R., Cook, E.R., Sano, M., Wichienkeo, A., Minh, A.A., Hong, T.M., 2010. Climate as a contributing factor in the demise of Angkor, Cambodia. *Proceedings of the National Academy of Sciences* 107, 6748-6752.
- Burns, S.J., Fleitmann, D., Mudelsee, M., Neff, U., Matter, A., Mangini, A., 2002. A 780-year annually resolved record of Indian Ocean monsoon precipitation from a speleothem from south Oman. *Journal of Geophysical Research: Atmosphere* 107.doi:10.1029/2001JD001281.
- Caulle, C., Koho, K.A., Mojtahid, M., Reichart, G.J., Jorissen, F.J., 2014. Live (Rose Bengal stained) foraminiferal faunas from the northern Arabian Sea: Faunal succession within and below the OMZ. *Biogeosciences* 11, 1155–1175.
- Chao, W.C., Chen, B., 2001. The origin of monsoons. *Journal of the Atmospheric Sciences* 58, 3497-3507.
- Charney, J.G., 1969. The intertropical convergence zone and the hadley circulation of the atmosphere. *Proc. WMO/IUCG Symposium Numerical Weather Prediction Japan Meteorological Agency III*, 73–79.
- Chauhan, O.S., 2003. Past 20,000-year history of Himalayan aridity: Evidence from oxygen isotope records in the Bay of Bengal. *Current Science* 84, 90-93.
- Clemens, S.C., Prell, W.L., 1991. One-million year record of summer-monsoon winds and continental aridity from the Owen Ridge (Site 722B), northwest Arabian Sea. *Ocean Drilling Program Scientific Results* 117, 365-388.

- Clift, P.D., Plumb, R.A., 2008. *The Asian Monsoon: Causes, History and Effectc.* Cambridge University Press, 270 p.
- Corliss, B.H., Chen, C., 1988. Morphotype patterns of Norwegian Sea deep-sea benthic foraminifera and ecological implications. *Geology* 16, 716-719.
- DeSousa, S.N., Dileepkumar, M., Sardessai, S., Sarma, V.V.S.S., Shirodkar, P.V., 1996. Seasonal variability in oxygen and nutrients in the central and eastern Arabian Sea. *Current Science* 71, 847-851.
- Dutta, K., Bhushan, R., Somayajulu, B.K., 2001. Delta R correction values for the northern Indian Ocean. *Radiocarbon* 43, 483-488.
- Fleitmann, D., Burns, S.J., Mangini, A., Mudelsee, M., Kramers, J., Villa, I., Neff, U., Al-Subbary, A.A., Buettner, A., Hippler, D., Matter, A., 2007. Holocene ITCZ and Indian monsoon dynamics recorded in stalagmites from Oman and Yemen (Socotra). *Quaternary Science Reviews* 26, 170-188.
- Gadgil, S., Abrol, Y.P., Rao, S.P., 1999. On growth and fluctuation of Indian foodgrain production. *Current Science* 76, 548-556.
- Gadgil, S., 2003. The Indian monsoon and its variability. *Annual Review of Earth and Planetary Sciences* 31, 429-467.
- Gadgil, S., Vinayachandran P.N., Francis, P.A., Gadgil, S., 2004. Extremes of the Indian summer monsoon rainfall, ENSO and equatorial Indian Ocean oscillation, *Geophysical Research Letters* 31, L12213, doi:10.1029/2004GL019733.
- Garcia, H. E., Locarnini, R.A., Boyer, T.P., Antonov, J.I., Baranova, O.K., Zweng, M.M., Johnson, D.R., 2010. *World Ocean Atlas 2009, Volume 3: Dissolved Oxygen, Apparent Oxygen Utilization, and Oxygen Saturation.* S. Levitus, Ed. NOAA Atlas NESDIS 70, U.S. Government Printing Office, Washington, D.C., 344 .
- Gomes, H.R., Goes J.I., Saino, T., 2000. Influence of physical processes and freshwater discharge on the seasonality of phytoplankton regime in the Bay of Bengal. *Continental Shelf Research* 20, 313-330.
- Goswami, B.N., 2006. The Asian monsoon: Interdecadal variability. *In* *The Asian Monsoon* (B. Wang Ed.), Springer Berlin.
- Gouretski, V.V., Koltermann, K.P., 2004. WOCE global hydrographic climatology. *Berichte des Bundesamtes für Seeschifffahrt und Hydrographie* 35, 52.
- Govil, P., Naidu, P.D., 2011. Variations of Indian monsoon precipitation during the last 32kyr reflected in the surface hydrography of the Western Bay of Bengal. *Quaternary Science Reviews* 30, 3871-3879.
- Gupta., A.K., Anderson, D.D.M., Overpeck, J.J.T., 2003. Abrupt changes in the Asian southwest monsoon during the Holocene and their links to the North Atlantic Ocean. *Nature* 421, 354–357.
- Gupta, A.K., Das, M., Anderson, D.M., 2005. Solar influence on the Indian summer monsson during the Holocene. *Geophysical Research Letters* 32, 1–4.

- Halley, E., 1686. An historical account of the trade winds and monsoons observable in the seas between and near the tropics with an attempt to assign a physical cause of the said winds. *Philosophical Transactions of the Royal Society of London, Series A* 16, 153–168.
- Henderson, G.M., 2002. New oceanic proxies for paleoclimate. *Earth and Planetary Science Letters* 203, 1–13.
- Kessarkar, P.M., Rao, V.P., Naqvi, S.W.A., Karapurkar, S.G., 2013. Variation in the Indian summer monsoon intensity during the Bolling-Allerod and Holocene. *Paleoceanography* 28, 413–425.
- Kudrass, H.R., Hofmann, A., Dooze, H., Emeis, K., Erlenkeuser, H., 2001. Modulation and amplification of climatic changes in the Northern Hemisphere by the Indian summer monsoon during the past 80 k.y. *Geology* 29, 63–66.
- Kumar, K.K., Rajagopalan, B., Cane, M.A., 1999. On the weakening relationship between the Indian monsoon and ENSO. *Science*, 284, 2156–2159.
- Levitus, S., Boyer, T.P., 1994. *World Ocean Atlas 1994. Temperature* (No. PB--95270112/XAB; NESDIS--4). National Environmental Satellite, Data, and Information Service, Washington, DC (United States).
- Locarnini, R.A., Mishonov, A.V., Antonov, J. I., Boyer, T. P., Garcia, H. E., Baranova, O. K., Zweng, M. M., Johnson, D.R., 2010. *World Ocean Atlas 2009, Volume 1: Temperature*. S. Levitus, Ed. NOAA Atlas NESDIS 68, U.S. Government Printing Office, Washington, D.C., 184 pp.
- Mahesh, B.S., Banakar, V.K., 2014. Change in the intensity of low-salinity water inflow from the Bay of Bengal into the Eastern Arabian Sea from the Last Glacial Maximum to the Holocene: Implications for monsoon variations. *Palaeogeography, Palaeoclimatology, Palaeoecology* 397, 31–37.
- Manasa, M., Saraswat, R., Nigam, R., 2016. Assessing the suitability of benthic foraminiferal morpho-groups to reconstruct paleomonsoon from Bay of Bengal. *Journal of Earth System Sciences* 125, 571–584.
- Mazumder, A., Nigam, R., 2014. Bathymetric preference of four major genera of rectilinear benthic foraminifera within oxygen minimum zone in Arabian Sea off central west coast of India. *Journal of Earth System Sciences* 123, 633–639.
- Milliman, J.D., 2001. Delivery and fate of fluvial water and sediment to the sea: a marine geologist's view of European rivers. *Scientia Marina* 65, 121–132.
- Mohtadi, M., Prange, M., Steinke, S., 2016. Palaeoclimatic insights into forcing and response of monsoon rainfall. *Nature* 533, 191–199.
- Nagy, J., Reolid, M., Rodriguez-Tovar, F.J., 2009. Foraminiferal morphogroups in dysoxic shelf deposits from the Jurassic of Spitsbergen. *Polar Research* 28, 214–221.
- Naidu, P.D., Malmgren, B.A., 1996. A high-resolution record of late Quaternary upwelling along the Oman Margin, Arabian Sea based on planktonic foraminifera. *Paleoceanography* 11, 129–140.

- Naqvi, S.W.A., Jayakumar, D.A., Narvekar, P.V., Naik, H., Sarma, V.V.S.S., D'souza, W., Joseph, S., George, M.D., 2000. Increased marine production of N₂O due to intensifying anoxia on the Indian continental shelf. *Nature* 408, 346-349.
- Nigam, R., Khare, N., Borole, D.V., 1992. Can benthic foraminiferal morpho-groups be used as indicators of paleomonsoonal precipitation?. *Estuarine, Coastal and Shelf Science* 34, 533-542.
- Nigam, R., Khare, N., Nair, R.R., 1995. Foraminiferal evidences for 77-year cycles of droughts in India and its possible modulation by the Gleissberg solar cycle. *Journal of Coastal Research* 11, 1099-1107.
- Nigam, R., Mazumder, A., Henriques, P.J., Saraswat, R., 2007. Benthic foraminifera as proxy for oxygen depleted conditions off the central west coast of India, *Journal of Geological Society of India* 70 1047–1054.
- Ostlund, H.G., Oleson, R., Brescher, R., 1980. GEOSECS Indian Ocean radiocarbon and tritium results. Tritium Laboratory Data Research, 9. University of Miami, Miami, Fla 15 pp.
- Panchang, R., Nigam, R., 2012. High resolution climatic records of the past ~489 years from Central Asia as derived from benthic foraminiferal species, *Asterorotalia trispinosa*. *Marine Geology* 307-310, 88–104.
- Phadtare, N.R., Pant, R.K., 2006. A century-scale pollen record of vegetation and climate history during the past 3500 years in the Pinder Valley, Kumaon Higher Himalaya, India. *Journal of Geological Society of India* 68, 495–506.
- Ponton, C., Giosan, L., Eglinton, T.I., Fuller, D. Q., Johnson, J.E., Kumar, P., Collett, T.S., 2012. Holocene aridification of India. *Geophysical Research Letters* 39, L03704.
- Prasanna Kumar, S., Nuncio, M., Narvekar, J., 2004. Are eddies nature's trigger to enhance biological productivity in the Bay of Bengal? *Geophysical Research Letters* 31, L07309.
- Prasanna Kumar, S.; Narvekar, J., Nuncio, M., Kumar, A., Ramaiah, N., Sardesai, S., Gauns, M., Fernandes, V., Paul, J., 2010. Is the biological productivity in the Bay of Bengal light limited? *Current Science* 98, 1331-1339.
- Ramaswamy, V., Nair, R.R., 1994. Fluxes of material in the Arabian Sea and Bay of Bengal- Sediment trap studies. *Proceedings of the Indian Academy of Sciences-Earth and Planetary Sciences* 103, 189-210.
- Rana, S., Nigam, R., 2009. Cyclicity in Late Holocene monsoonal changes from the western Bay of Bengal: Foraminiferal approach. *Journal of the Palaeontological Society of India* 54, 165-170.
- Rao, C.K., Naqvi, S.W.A., Kumar, M.D., Varaprasad, S.J.D., Jayakumar, D.A., George, M.D., Singbal, S.Y.S., 1994. Hydrochemistry of the Bay of Bengal: possible reasons for a different water-column cycling of carbon and nitrogen from the Arabian Sea. *Marine Chemistry* 47, 279-290.
- Rashid, H., England, E., Thompson, L., Polyak, L., 2011. Late glacial to Holocene Indian summer monsoon variability based upon sediment. *Terrestrial Atmospheric and Oceanic Sciences* 22, 215-228.

- Reimer, P.J., Baillie, M.G.L., Bard, E., Bayliss, A., Beck, J.W., Blackwell, P.G., Ramsey, C.B., Buck, C.E., Burr, G.S., Edwards, R.L., Friedrich, M., Grootes, P.M., Guilderson, T.P., Hajdas, I., Heaton, T.J., Hogg, A.G., Hughen, K.A., Kaiser, K.F., Kromer, B., McCormac, F.G., Manning, S.W., Reimer, R.W., Richards, D.A., Southon, J.R., Talamo, S., Turney, C.S.M., van der Plicht, J., Weyhenmeyer, C.E., 2013. Intcal13 and Marine13 radiocarbon age calibration curves, 0-50,000 years cal BP. *Radiocarbon* 55, 1869-1887.
- Saraswat, R. 2015. Non-destructive foraminiferal paleoclimatic proxies: A brief insight. *Proceedings Indian National Science Academy* 81, 381-395.
- Saraswat, R., Nigam, R., Barreto, L. 2005. Paleoceanographic implications of abundance and mean proloculus diameter of benthic foraminiferal species *Epistominella exigua* in sub-surface sediments from distal Bay of Bengal Fan. *Journal of Earth System Sciences* 114, 453-458.
- Saraswat, R., Nigam, R., Mackensen, A., Weldeab, S., 2012. Linkage between seasonal insolation gradient in the tropical northern hemisphere and the sea surface salinity of the equatorial Indian Ocean during the last glacial period. *Acta Geologica Sinica* 86, 801-811.
- Saraswat, R., Lea, D.W., Nigam, R., Mackensen, A., Naik, D.K., 2013. Deglaciation in the tropical Indian Ocean driven by interplay between the regional monsoon and global teleconnections. *Earth and Planetary Science Letters* 375, 166-175.
- Saraswat, R., Nigam, R., Correge, T., 2014. A glimpse of the Quaternary monsoon history from India and adjoining seas. *Palaeogeography Palaeoclimatology Palaeoecology* 397, 1-6.
- Saraswat, R., Naik, D.K., Nigam, R., Gaur, A.S., 2016. Timing, cause and consequences of mid-Holocene climate transition in the Arabian Sea. *Quaternary Research* 86, 162-169.
- Sardessai, S., Ramaiah, N., Kumar, P., Sousa, D., 2007. Influence of environmental forcings on the seasonality of dissolved oxygen and nutrients in the Bay of Bengal. *Journal of Marine Research* 65, 301-316.
- Schlitzer R., 2016. Ocean Data View; <http://odv.awi.de>
- Schulz, M., Mudelsee, M., 2002. REDFIT: estimating red-noise spectra directly from unevenly spaced paleoclimatic time series. *Computers & Geosciences* 28, 421-426.
- Schumacher, S., Jorissen, F.J., Dissard, D., Larkin, K.E., Gooday, A.J., 2007. Live (Rose Bengal stained) and dead benthic foraminifera from the oxygen minimum zone of the Pakistan continental margin (Arabian Sea). *Marine Micropaleontology* 62, 45-73.
- Sen Gupta, B.K., Machain-Castillo, M.L., 1993. Benthic foraminifera in oxygen-poor habitats. *Marine Micropaleontology* 20, 3-4.
- Severin, K.P., 1983. Test morphology of benthic foraminifera as a discriminator of biofacies. *Marine Micropaleontology* 8, 65-76.
- Sijinkumar, A.V., Clemens, S., Nath, B.N., Prell, W., Benschila, R., Lengaigne, M., 2016. $\delta^{18}\text{O}$ and salinity variability from the Last Glacial Maximum to Recent in the Bay of Bengal and Andaman Sea. *Quaternary Science Reviews* 135, 79-91.

- Singh, A.D., Jung, S. J. A., Darling, K., Ganeshram, R., Ivanochko, T., Kroon, D., 2011. Productivity collapses in the Arabian Sea during glacial cold phases. *Paleoceanography* 26, PA3210, doi:10.1029/2009PA001923.
- Singh, A.D., Rai, A.K., Verma, K., Das, S., Bharti, S.K. 2014. Benthic foraminiferal diversity response to the climate induced changes in the eastern Arabian Sea oxygen minimum zone during the last 30 ka BP. *Quaternary International*
- Sinha, A., Cannariato, K.G., Stott, L.D., Cheng, H., Edwards, R.L., Yadava, M.G., Ramesh, R., Singh, I.B., 2007. A 900-year (600 to 1500 A.D.) record of the Indian summer monsoon precipitation from the core monsoon zone of India. *Geophysical Research Letters* 34, 1–5.
- Sirocko, F., Sarnthein, M., Erlenkeuser, H., Lange, H., Arnold, M., Duplessy, J.C., 1993. Century-scale events in monsoonal climate over the past 24,000 years. *Nature* 364, 322-324.
- Staubwasser, M., Weiss, H. 2006. Holocene climate and cultural evolution in late prehistoric–early historic West Asia. *Quaternary Research* 66, 372–387.
- Stuiver, M., Reimer, P.J., and Reimer, R.W., 2016, CALIB 7.1 [WWW program] at <http://calib.org>.
- Southon, J., Kashgarian, M., Fontugne, M., Metivier, B., & Yim, W.W., 2002. Marine reservoir corrections for the Indian Ocean and Southeast Asia. *Radiocarbon* 44, 167-180.
- Tiwari, M., Ramesh, R., Somayajulu, B. L. K., Jull, A. T., Burr, G. S., 2005. Solar control of southwest monsoon on centennial timescales. *Current Science* 89, 1583.
- Varkey, M.J., Murty, V.S.N., Suryanarayana, A., 1996. Physical oceanography of the Bay of Bengal and Andaman Sea. *Oceanography and Marine Biology: An Annual Review* 34, 1-70.
- Wang, Y.J., Cheng, H., Edwards, R.L., He, Y.Q., Kong, X.G., An, Z.S., Wu, J.Y., Kelly, M.J., Dykoski, C.A., Li, X.D., 2005. The Holocene Asian monsoon: Links to solar changes and North Atlantic climate. *Science* 308, 854–857.
- Wang, B., Huang, F., Wu, Z., Yang, J., Fu, X., Kikuchi, K., 2009. Multi-scale climate variability of the South China Sea monsoon: A review. *Dynamics of Atmosphere and Ocean* 47, 15–37.
- Wyrtki, K., 1971. *Oceanographic Atlas of the International Indian Ocean Expedition*. National Science Foundation., Washington, DC, 531.
- Zhang, P., Cheng, H., Edwards, R. L., Chen, F., Wang, Y., Yang, X, Liu, et al., An, C., 2008. A test of climate, sun, and culture relationships from an 1810-year Chinese cave record. *Science* 322, 940-942.

Legend to Figures and Tables

- Figure 1: Location of surface sediment samples (black-filled inverted triangles) and gravity core (green filled square). The contour are bathymetry in meters. The location of major rivers is marked on the map. The study area in the northern Indian Ocean is marked by the black rectangle in the inset.
- Figure 2: Salinity (psu) (A), dissolved oxygen (ml/l) B) and temperature (°C) at the sediment water interphase in the western Bay of Bengal. The plots are based on the measurements made on water retrieved in multi-core tops, augmented with the data downloaded from world ocean atlas (Levitus et al., 1994; Locarnini et al., 2010).
- Figure 3: Distribution of C_{org} (%) in surface sediments of the central-western Bay of Bengal. The locations of surface sediment samples are marked by inverted black triangles. The bathymetric contours are marked by thin black lines labelled in meters. The major rivers draining in the western Bay of Bengal are also marked on the map.
- Figure 4: Distribution of coarse fraction in the study area. The bathymetric contours are labelled in meters. The scale is in percentage. The major rivers draining in the western Bay of Bengal are also marked on the map. Black filled inverted triangles are the surface sediment locations.
- Figure 5: Representative angular asymmetrical (A-H) and rounded symmetrical (I-P) benthic foraminiferal genera. A. *Hormosina*, B. *Reophax*, C. *Astacolus*, D. *Brizalina*, E. *Bolivina*, F. *Cassidelina*, G. *Bulimina*., H. *Uvigerina*, I. *Rosalina*, J. *Hyalinea*, K. *Ammonia*, L. *Cibicides*, M. *Discorbinella*, N. *Ammodiscus*, O. *Amphistegina*, P. *Asterorotalia*. The scale bar is 100 μm , unless otherwise mentioned.
- Figure 6: Surface distribution of relative abundance of benthic foraminiferal morpho-groups. A. Fossil angular asymmetrical benthic foraminifera (AABF); B. Fossil rounded symmetrical benthic foraminifera (RSBF); C. Living AABF; D. Living RSBF. The scale is in percentage.
- Figure 7: Principal Component Analysis biplot of morpho-groups and environmental data. The red squares with the red dashed lines denote the morpho-groups while the blue circles with blue dashed lines denote the environmental data.

Figure 8: Down-core variation in coarse fraction abundance (%) and relative abundance of both the angular asymmetrical benthic foraminifera (AABF) and rounded symmetrical benthic foraminifera (RSBF). The grey line is the original data and the thick black line is 3-point running average. The age of the sediments has been established from AMS ¹⁴C dates.

Figure 9: Broad trends in down-core changes in relative abundance of angular asymmetrical benthic foraminifera (AABF). The grey line is the original data and the thick black line is 3-point running average. The blue line marks the decrease in AABF abundance suggesting stronger monsoon during Medieval Warm Period (MWP) and the red line indicates a progressive increase in AABF abundance suggesting weaker monsoon during Little Ice Age (LIA).

Figure 10: Result of spectral analysis of temporal changes in relative abundance of angular asymmetrical benthic foraminifera in core. The periodicity at various confidence intervals is also marked.

Table 1: Details of surface samples. The coarse fraction percentage and relative abundance of both the fossil and living angular asymmetrical (AABF) and rounded symmetrical benthic foraminifera (RSBF) is also given.

Table 2: Details of the core location used to reconstruct past monsoon changes during the last ~2000 years.

Table 3: Details of ¹⁴C accelerator mass spectrometer dates on core SK308 GC-02.

Table 4: Details of the correlation analysis. Marked correlations in red, are significant at $p < 0.0500$.

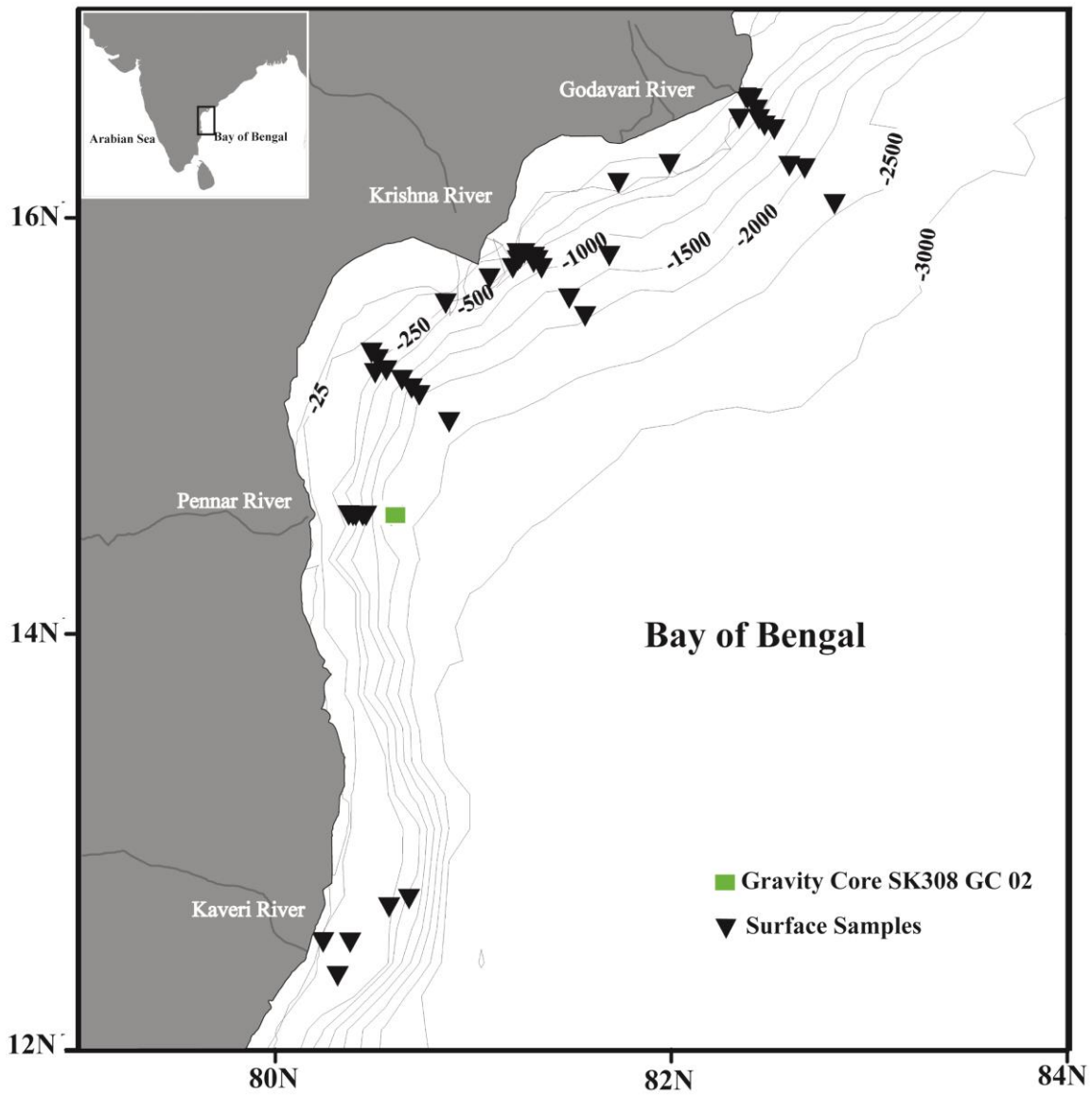


Figure 1

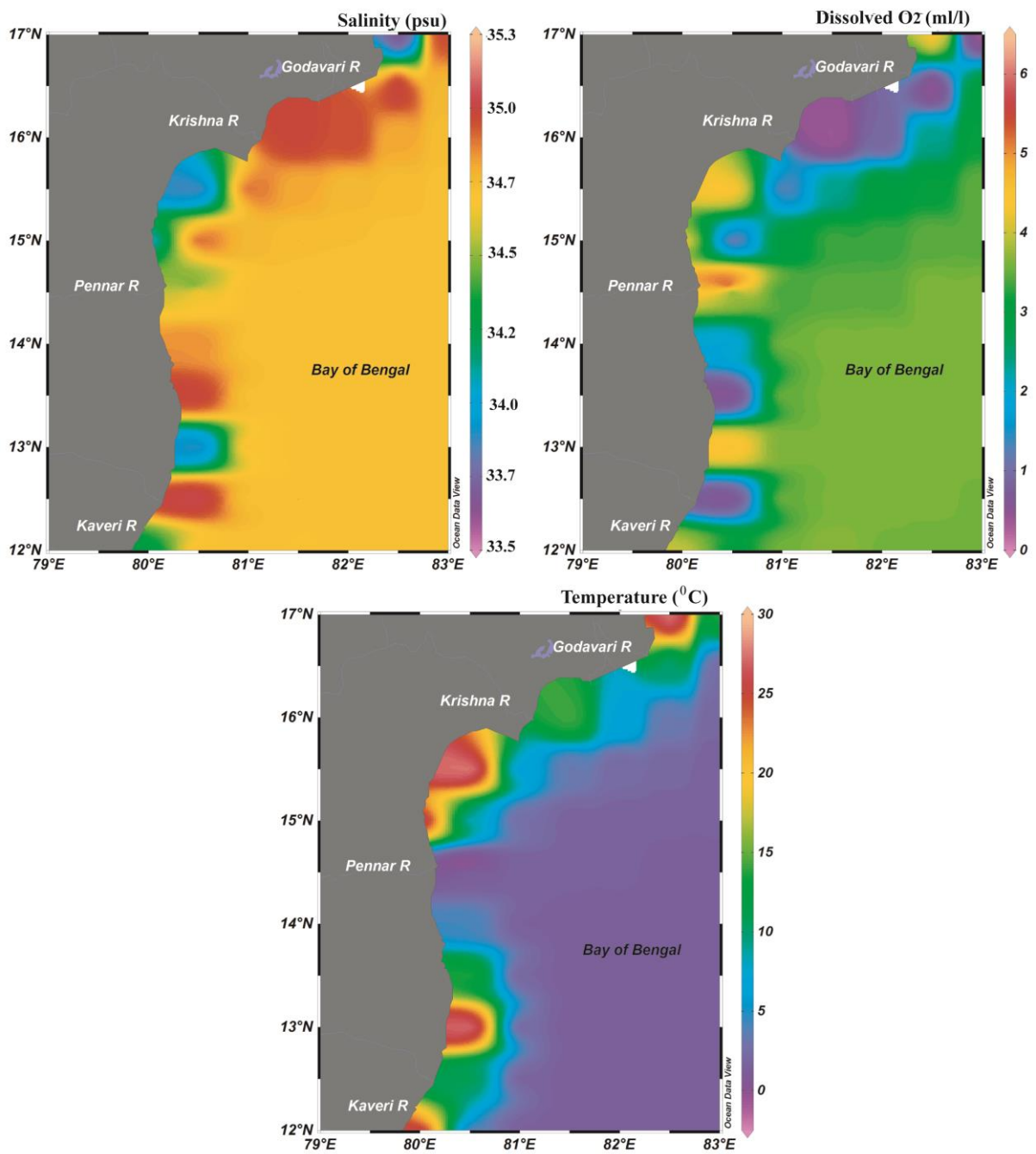


Figure 2

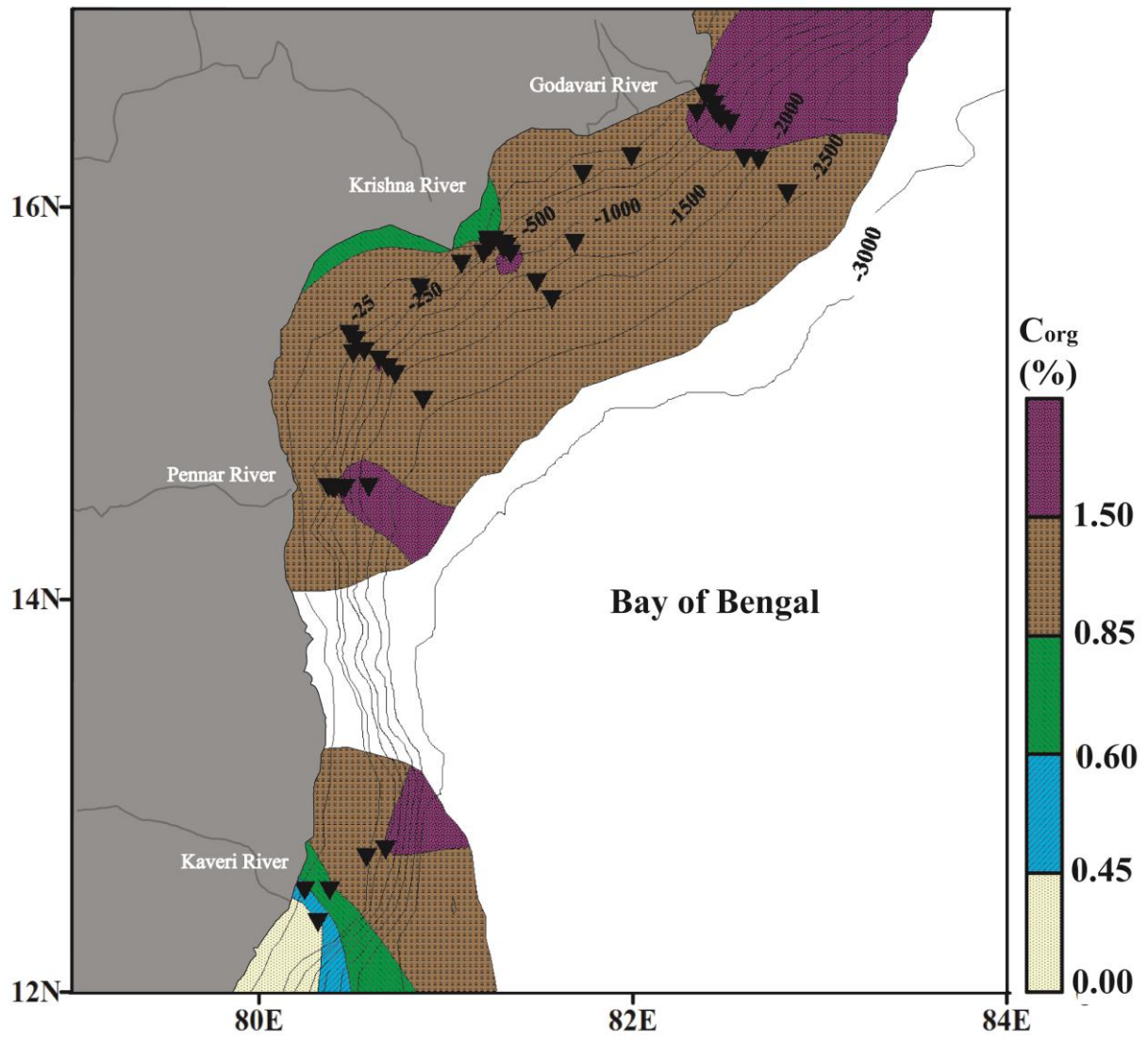


Figure 3

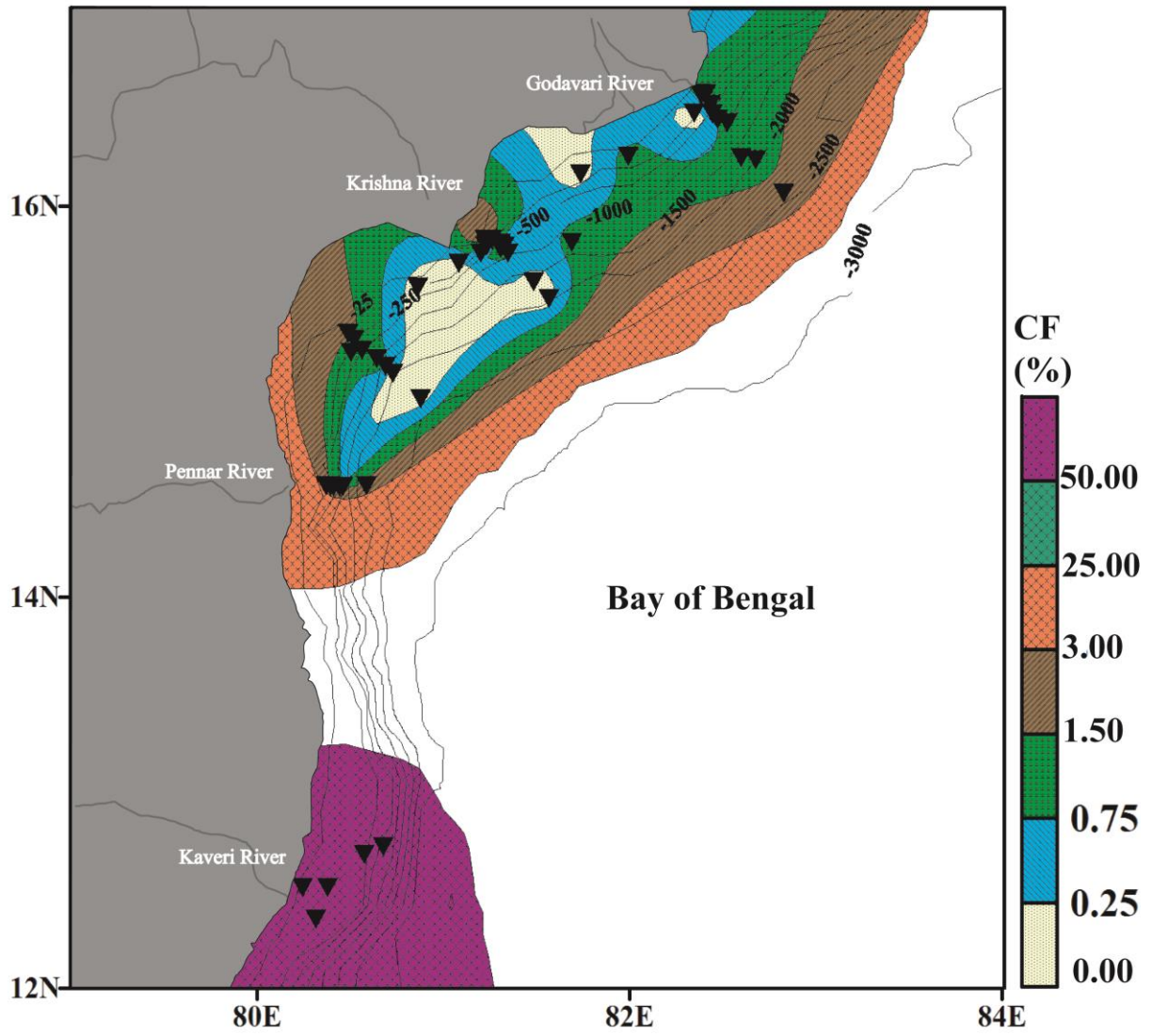


Figure 4

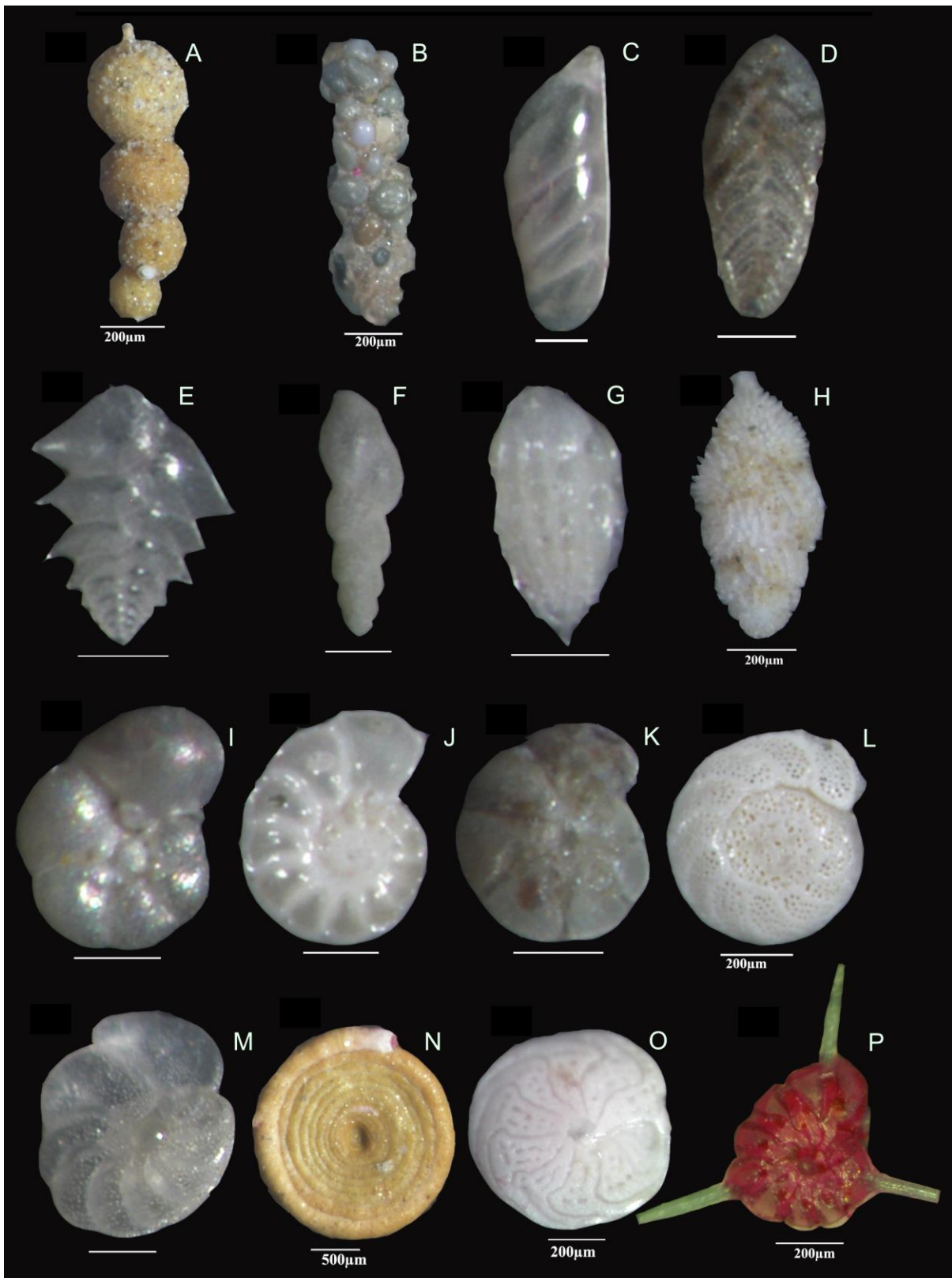


Figure 5

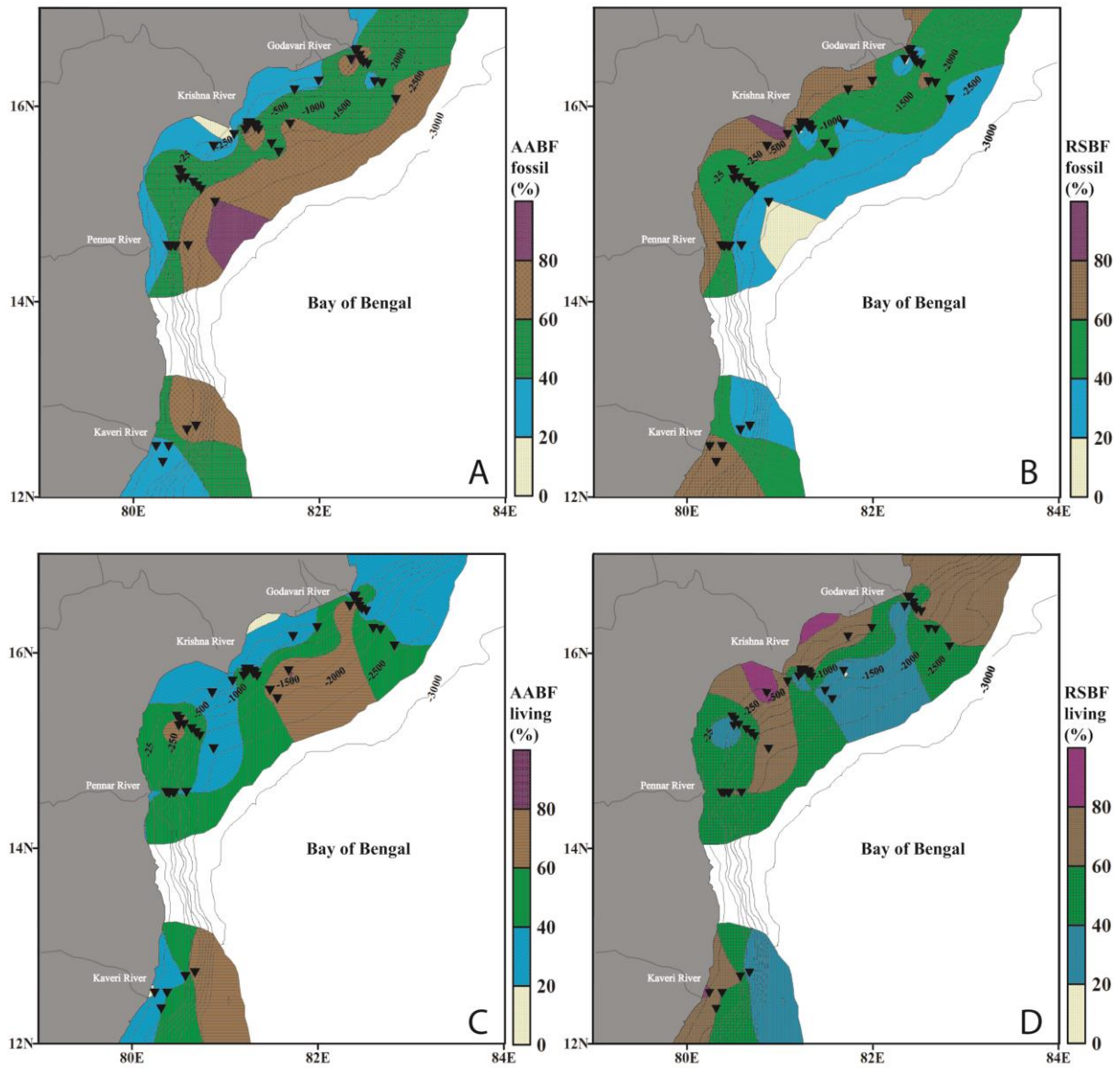


Figure 6

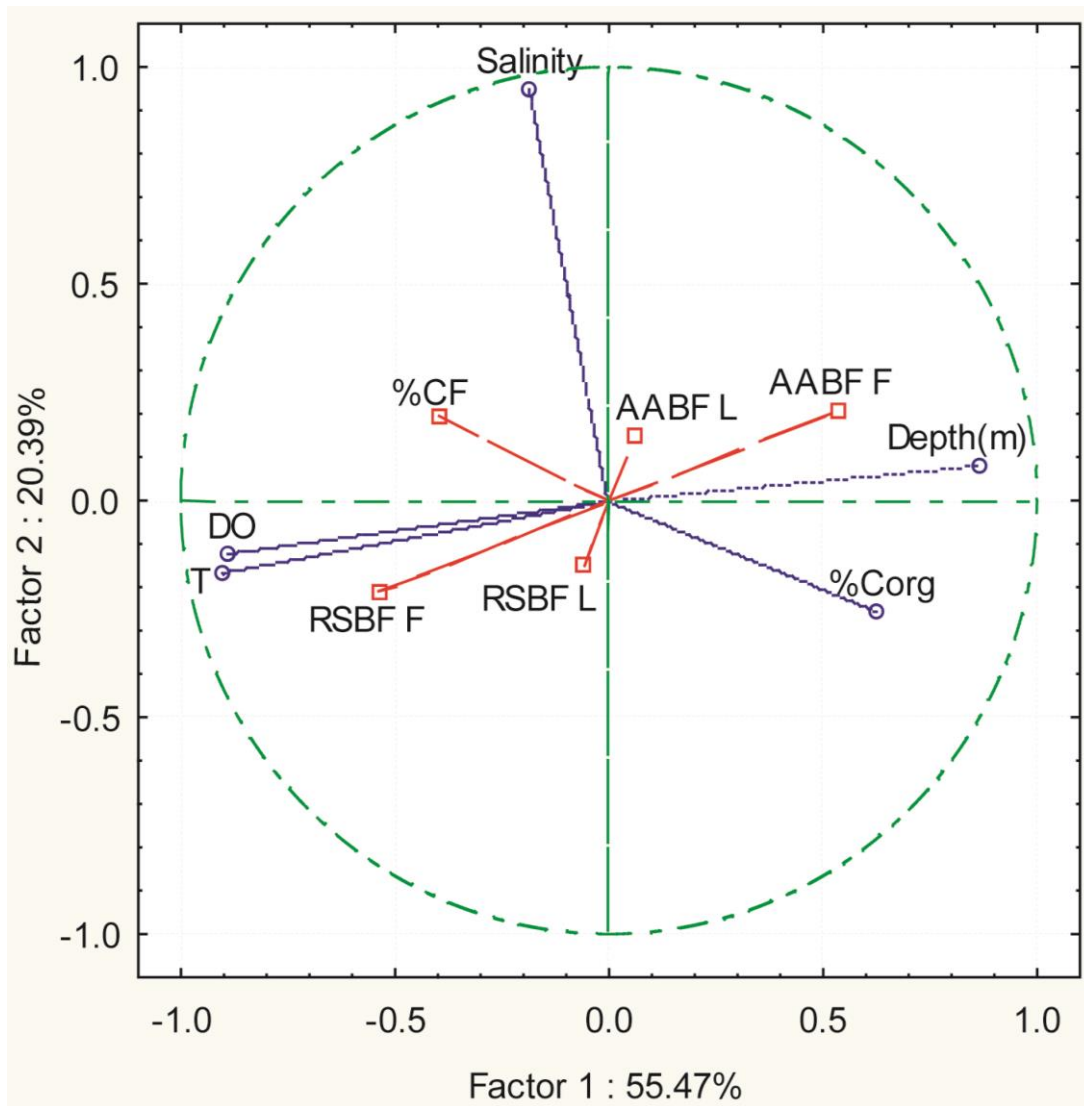


Figure 7

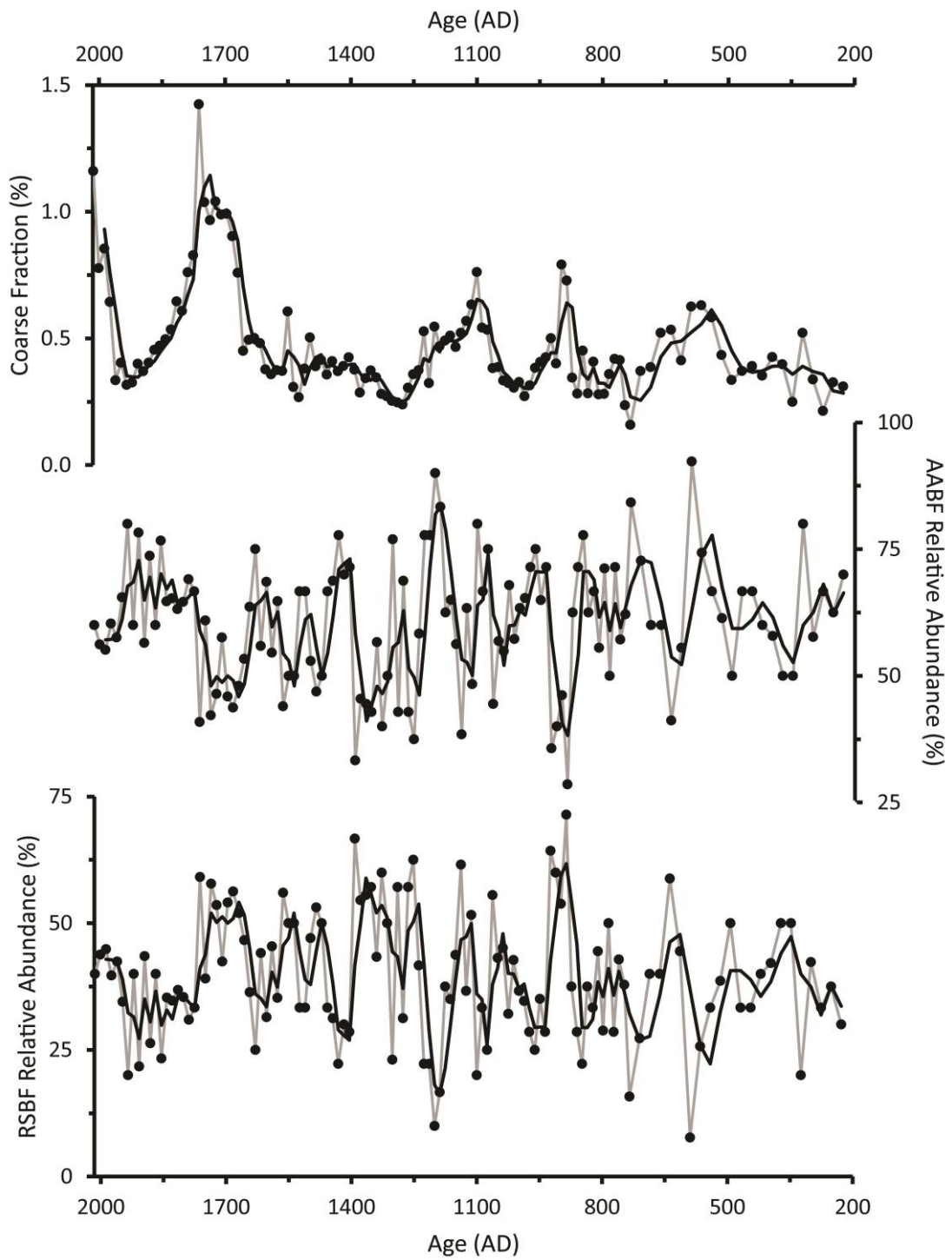


Figure 8

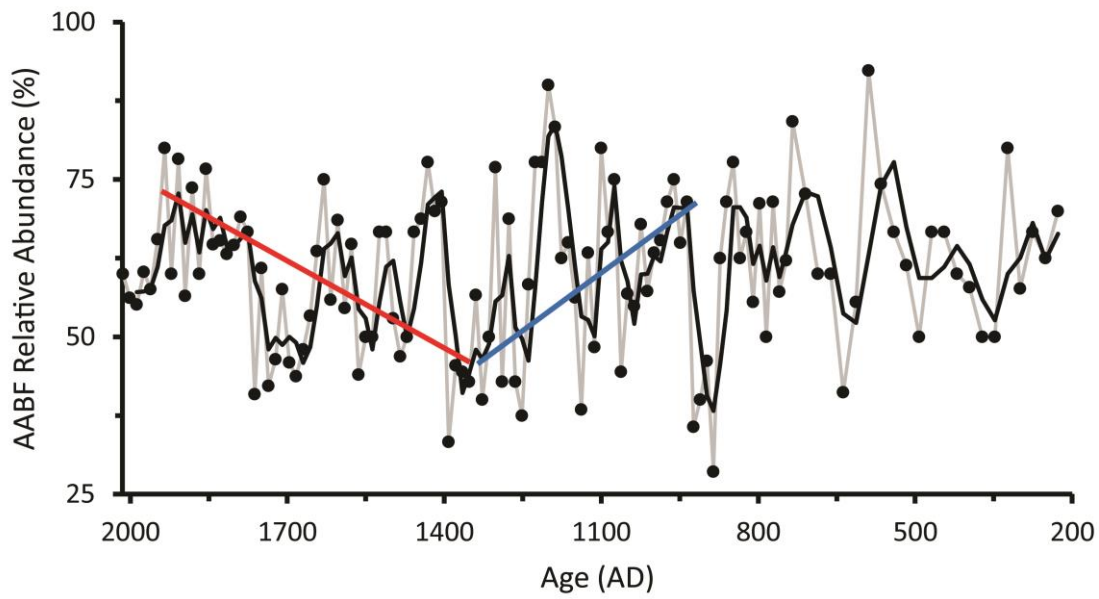


Figure 9

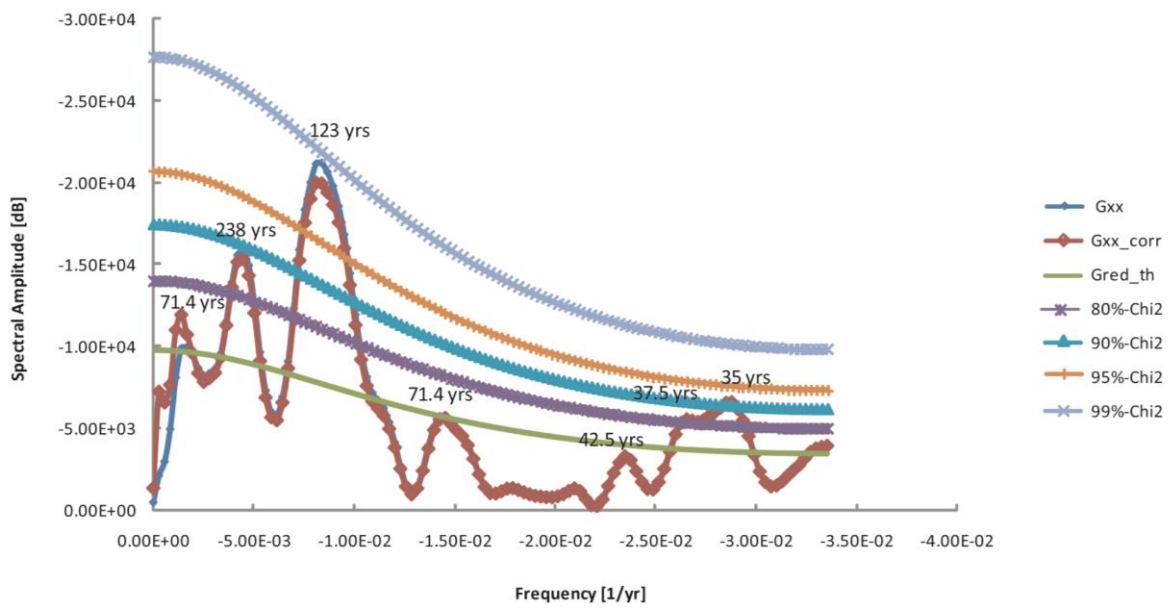


Figure 10

Table 1:

Sample Name	Long (°E)	Lat (°N)	Depth (m)	Coarse Fraction (%)	Fossil RSBF (%)	Fossil AABF (%)	Living RSBF (%)	Living AABF (%)
MC-02	80.59	14.57	2090.0	1.5	26	74	60	40
MC-03	80.46	14.57	1476.0	1.5	29	71	64	36
MC-04	80.44	14.57	978.5	0.4	45	55	0	100
MC-05	80.41	14.57	396.6	1.1	36	64	20	80
MC-06	80.39	14.57	243.8	1.1	45	55	29	71
MC-07	80.37	14.57	47.0	3.4	75	25	61	39
MC-08	80.49	15.35	76.0	1.9	42	58	45	55
MC-09	80.52	15.32	274.0	0.5	15	85	23	77
MC-11	80.56	15.27	500.3	0.8	63	37	48	52
MC-12	80.50	15.25	785.9	0.6	39	61	21	79
MC-13	80.64	15.22	921.0	0.7	41	59	42	58
MC-14	80.69	15.18	1518.8	0.7	42	58	54	46
MC-15	80.73	15.15	1940.4	0.4	31	69	55	45
MC-16	80.88	15.02	2481.6	0.4	10	90	72	28
MC-18	81.56	15.53	2005.6	0.3	20	80	38	62
MC-19	81.48	15.61	1463.0	0.4	31	69	35	65
MC-20	81.35	15.76	1069.0	0.7	15	85	55	45
MC-21	81.32	15.80	749.2	0.4	27	73	60	40
MC-22	81.30	15.78	767.8	0.7	21	79	74	26
MC-23	81.31	15.81	507.3	0.3	49	51	69	31
MC-24	81.20	15.76	202.0	0.9	6	94	5	95
MC-25	81.24	15.80	79.5	1.1	33	67	48	52
MC-26	81.23	15.79	102.6	0.4	15	85	14	86
MC-27	81.69	15.82	55.1	1.4	31	69	17	83
MC-28	81.22	15.83	31.6	2.9	65	35	62	38
MC-29	82.38	16.58	27.3	1.3	76	24	81	19
MC-30	82.39	16.57	40.0	0.7	55	45	90	10
MC-31	82.41	16.57	107.3	1.1	29	71	37	63
MC-32	82.43	16.52	259.3	0.6	3	97	17	83
MC-33	82.44	16.47	495.6	0.5	38	62	48	52
MC-34	82.47	16.44	744.4	0.7	33	67	81	19
MC-35	82.52	16.42	1005.8	0.5	57	43	77	23
MC-36	82.60	16.25	1511.1	0.7	73	27	43	57
MC-37	82.67	16.24	1980.6	0.7	14	86	56	44
MC-38	82.82	16.06	2494.9	1.5	8	92	59	41
SC-36	82.34	16.48	145.0	0.2	5	95	5	95
SC-37	81.99	16.26	44.0	1.5	63	37	60	40
SC-38	81.73	16.17	52.0	0.3	58	42	76	24

SC-39	81.26	15.83	62.0	1.8	54	46	75	25
SC-40	81.08	15.71	53.0	0.5	87	13	68	32
SC-41	80.86	15.59	69.0	0.1	70	30	78	22
SC-42	80.31	12.35	56.0	96.4	71	29	60	40
SC-43	80.38	12.52	52.0	94.8	58	42	56	44
SC-44	80.24	12.52	33.0	71.5	64	36	83	17
SC-45	80.57	12.68	107.0	94.2	22	78	67	33
SC-46	80.67	12.72	190.0	66.6	26	74	20	80

Table 2:

Core	Water depth (m)	Latitude (°N)	Longitude (°E)
SK308 GC-02	2094	14°34.115	80°35.112

Table 3:

Lab Code	Sample Interval (cm)	¹⁴ C age (yr BP)	Calibrated Age (Median Probability) (yr BP)
UGAMS23864	48-50	1170	649
UGAMS23865	98-100	1830	1280
UGAMS23866	185-187	3610	3381

Table 4:

Variable	%CF	AABF F	RSBF F	RSBF L	AABF L
Depth	-0.27	0.49	-0.49	0.06	-0.06
Salinity	0.21	0.17	-0.17	-0.19	0.19
Temperature	0.32	-0.52	0.52	0.22	-0.22
Dissolved Oxygen	0.30	-0.37	0.37	-0.08	0.08
%C _{org}	-0.43	0.49	-0.49	-0.20	0.20